Journal of Materials Chemistry B

RSC Publishing

PAPER

View Article Online
View Journal | View Issue

Cite this: J. Mater. Chem. B, 2013, 1, 1903

A fluorogenic monolayer to detect the co-immobilization of peptides that combine cartilage targeting and regeneration†

Jordi Cabanas-Danés,[a] Carlo Nicosia,[a] Ellie Landman,[b] Marcel Karperien,[b] Jurriaan Huskens*[a] and Pascal Jonkheijm*[a]

Strategies to generate platforms combining tissue targeting and regeneration properties are in great demand in the regenerative medicine field. Here we employ an approach to directly visualize the immobilization of cysteine-terminated peptides on a novel fluorogenic surface. Peptides with relevant biological properties, CLPLGNSH and CLRGRYW, were synthesized to function as peptide binders to transforming growth factor (TGF)-β1 and collagen type II (CII). The selective immobilization of the peptides was directly detected using a fluorogenic surface. Adhered proteins were confined to patterns of these peptides matching with the fluorogenic areas. These results show that the fluorogenic signal can be used to detect the chemo-selective immobilization of non-fluorescent biomolecules and to correlate the cell response with the patterned peptides. After analyzing the sequence specificity and cross-reactivity of the binding of TGF-β1 and CII to the respective peptide regions employing immunofluorescence assays, both peptides were co-immobilized in a step-wise process as detected by the fluorogenic surface. TGF-β1 and CII could be self-sorted from a mixture in a regio-selective manner resulting in a bi-functional protein platform. Surfaces of CLPLGNSH pre-loaded with TGF-β1 showed excellent bioactivity in combination with human articular chondrocytes (HACs) and stimulated expression of chondrogenic markers.

Received 28th November 2012
Accepted 30th January 2013

DOI: 10.1039/c3tb20109k

www.rsc.org/MaterialsB

Introduction

Designing functional materials that combine both targeting and regenerating properties is desired to improve the properties of biomaterials commonly used in the regenerative medicine field. In particular, articular cartilage regeneration will greatly benefit from such dual material platforms because damaged cartilage shows restricted abilities to effectively form new tissue maintaining the native structural and mechanical properties.[1]

Employing peptides with specific targeting and regenerative properties is an effective strategy to induce specifically designed biological functions. Such peptides are often detected employing phage display technology, which allows for rapid screening of thousands of peptide sequences to interact with specific target proteins.[2] Taking advantage of this approach, Stupp *et al.* functionalized the periphery of peptide amphiphiles[3] with specific peptide sequences having regenerative properties for different clinical situations.[4] For example, when such functionalized peptide amphiphiles were able to capture transforming growth factors (TGF)-β1, successfully regenerated articular cartilage was found in a full thickness chondral defect in a rabbit model.[4a] In another report by Hubbel *et al.* cartilage targeting was elegantly demonstrated using polymeric nanoparticles that were functionalized with a specific peptide sequence with high affinity for collagen type 2, a major component of the cartilaginous matrix.[5]

Functionalization of surfaces with peptides is a widely explored strategy to increase the biological properties of a wide variety of biomaterials that lack intrinsic mechanisms to stimulate tissue formation. Current methods do not allow easy ways of examining the functionalization process. Here we present a novel strategy that allows the visualization of the immobilization products using fluorescence microscopy. In this approach, a biomaterial surface is first to be covered with a linker consisting of a fluorogenic molecule. In this study we demonstrate a proof of principle using glass as a model surface and show the general applicability of the method by preparing a bifunctional peptide platform for targeting of collagen type II (CII)[6] and delivery of TGF-β1, which maintains articular cartilage cells in its differentiated phenotype[7] while inducing chondrogenic

[a]Molecular Nanofabrication Group, MESA+ Institute for Nanotechnology and Faculty of Science and Technology, University of Twente, Enschede, The Netherlands. E-mail: j.huskens@utwente.nl; p.jonkheijm@utwente.nl; Tel: +31-534892987

[b]Developmental BioEngineering, MIRA Institute for Biomedical Technology and Technical Medicine, Faculty of Science and Technology, University of Twente, Enschede, The Netherlands

† Electronic supplementary information (ESI) available: Detailed description of materials, peptide synthesis, substrate and monolayer preparation, printing experiments, assays, the cell differentiation study and Fig. S1. See DOI: 10.1039/c3tb20109k

differentiation in bone marrow mesenchymal progenitor cells.[8] For this purpose, we used our previously reported self-reporting fluorogenic reactive monolayer[9] that allows direct visualization of the immobilization of cysteine-terminated peptides such as CGRGDS by a Michael addition reaction.[9,10] Using these fluorogenic surfaces yields a fast, simple, sensitive and non-destructive detection of the immobilization products upon direct visualization of the modified area using fluorescence microscopy. Fluorogenic reporting methods overcome the use of expensive and time-consuming labeling of compounds. A TGF-β1 binding peptide CLPLGNSH[4a] and a CII binding peptide CLRGRYW[5] were co-immobilized as detected by fluorescence microscopy. These dual platforms were subsequently used to bind TGF-β1 and collagen type II yielding a platform with regenerative and targeting properties, respectively. Finally, the activity of TGF-β1 tethered onto a layer of CLPLGNSH was tested on human articular chondrocytes (HACs) reporting an increased glycosaminoglycans (GAG) production.

Results and discussion

Immobilization strategy of peptides

For the fabrication of a fluorogenic platform, glass slides were first modified with an azide-terminated self-assembled monolayer (SAM) (Scheme 1 and ESI†).[11] Then, alkyne-functionalized fluorogenic coumarin **1** was immobilized *via* a Huisgen 1,3-dipolar cycloaddition reaction[12] by performing a 1 h reactive microcontact printing (μCP) step employing an oxidized polydimethylsiloxane (PDMS) stamp. The stamps were inked with a solution of coumarin **1**, Cu(I)$(CH_3CN)_4PF_6$ and tris[(1-benzyl-1*H*-1,2,3-triazol-4-yl)methyl]amine (TBTA). The presence of a methyl-4-oxo-2-butenoate group adjacent to the coumarin allows reaction with thiols and quenches the coumarin emission prior to reaction with such thiols.[9,13] Owing to this quenching, upon printing of **1**, the fluorescence of the pattern was almost indistinguishable from the background.[9] Subsequently, onto this self-reporting platform the covalent immobilization of cysteine-terminated peptides was performed by means of the Michael addition to the methyl-4-oxo-2-butenoate moiety of **1** yielding a fluorescent coumarin moiety (Scheme 1).

To establish the method for the immobilization of cysteine-modified peptides on the self-reporting surfaces, peptides were synthesized (ESI†) *via* solid phase peptide synthesis (SPPS) carrying an N-terminal cysteine (Scheme 1). The peptides have proven biological properties such as the binding of transforming growth factor (TGF-) β1 (CLPLGNSH, **2**)[4a,14] and binding to CII (CLRGRYW, **3**).[5] As a control for the specificity of the immobilization reaction, a peptide was synthesized in which the cysteine was replaced by methionine. As a control for the specific binding of proteins to the immobilized peptides, two scrambled peptides were synthesized (CHNLGLPS, **2′**, and CWRGLRY, **3′**).

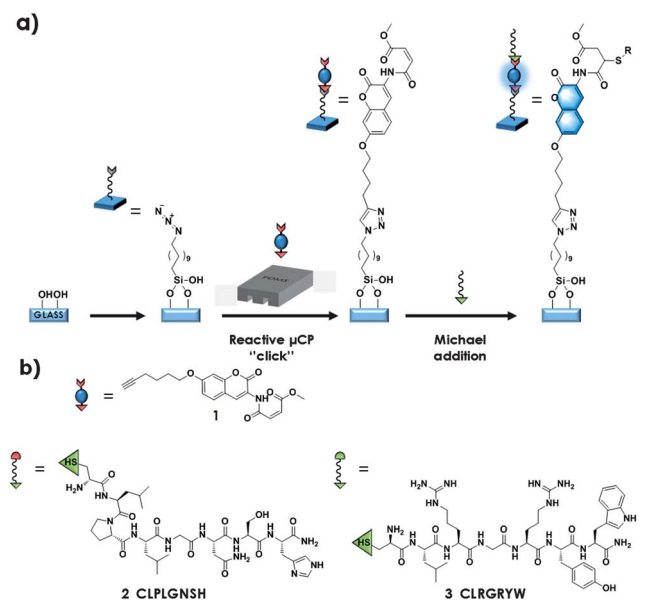

Scheme 1 (a) Signaled peptide immobilization strategy consisting of the reactive μCP of coumarin **1** on an azide-terminated SAM, followed by the covalent immobilization and detection of cysteine-terminated peptides by means of the fluorogenic Michael addition reaction to the methyl-4-oxo-2-butenoate moiety. (b) Chemical structures of the peptides employed in this work.

Detected co-immobilization of CLPLGNSH and CLRGRYW and binding of TGF-β1 and collagen type II

Incubating fluorogenic platforms with a solution of **2** or **2′** in PBS yielded an 8-fold enhancement of the coumarin fluorescence (Fig. 1a) while the intensity enhancement upon incubation with a solution of **3** or **3′** in PBS : DMSO (1 : 3) was *ca.* 6-fold

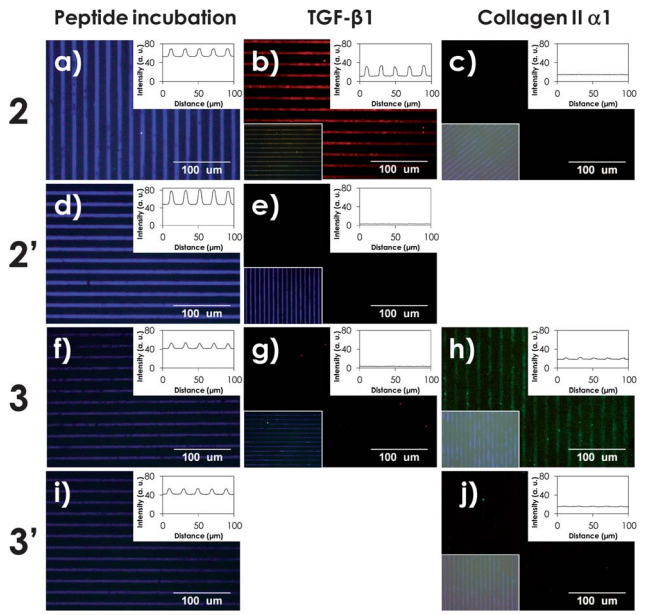

Fig. 1 Fluorescence images corresponding to substrates patterned with coumarin **1** after 1 h incubation with (a) **2**, (d) **2′**, (f) **3** and (i) **3′** and (b, e and g) after 1 h incubation with 1 μg mL^{-1} TGF-β1 and immunofluorescence staining (red) or (c, h and j) after 1 h incubation with collagen type II and immunofluorescence staining (green). Insets provide both intensity profiles and images captured using the blue channel while the main picture was recorded using either the red or the green channel.

(Fig. 1d). The intensity of the sample incubated in a solution containing the corresponding methionine derivative remained almost indistinguishable from the background and unchanged with respect to **1** (see ESI Fig. S1†). When the fluorogenic platform was incubated with cysteine ethyl ester an 8-fold enhancement of the coumarin fluorescence was observed relative to **1** (see Fig. S1b†). These results indicate that the peptide immobilization proceeds exclusively *via* the thiol of the cysteine-containing peptides and, in addition, when assuming full coverage for a small thiol-terminated molecule such as in the case of cysteine ethyl ester, a close-packed surface was found in the case of the cysteine end-capped peptide **2** while in the case of **3** a lower surface density of *ca.* 75% was found at the same time of incubation. Differences in the surface coverage could be related to differences in the solubility of the peptide and peptide structure.

After incubation of platforms functionalized with the CLPLGNSH (**2**) peptide in a solution containing TGF-β1 (1 μg mL^{-1}) in PBS for 1 h, an immunofluorescence assay (see ESI†) was performed to visualize the binding of TGF-β1 to the immobilized peptide. First a primary antibody was incubated for 1 h followed by an incubation of a secondary antibody labeled with a fluorescent dye for 1 h. After rinsing, the substrates were analyzed using fluorescence microscopy showing clearly red fluorescent patterns that coincide with the coumarin patterns (Fig. 1a and b). When this assay was performed on substrates functionalized with a scrambled peptide sequence (**2′**) (Fig. 1d and e) or with an unrelated peptide sequence (**3**) (Fig. 1f and g) no red fluorescent patterns could be discerned while the blue fluorescence was retained.

Another series of experiments were performed on platforms of peptide CLRGRYW (**3**). After incubating these platforms with bovine collagen type II (BCII) (50 μg mL^{-1}) an immunofluorescence assay (ESI†) was performed. After sequential incubation with primary and secondary antibodies, green fluorescent lines were observed using fluorescence microscopy indicative of the successful binding of BCII to the immobilized peptide **3** (Fig. 1f and h). Whereas the green fluorescent lines were excellently confined to patterns of **3**, minimal binding of BCII was detected on patterns of scrambled peptide sequence **3′** (Fig. 1i and j). In addition, the binding of BCII was absent on patterns of the TGF-β1 peptide **2** indicating negligible cross-reactivity among sequences (Fig. 1c). These results show that (i) the binding of TGF-β1 and BCII is sequence specific and selective, and (ii) bound TGF-b1 and BCII retain their structural integrity.

Having these results in hand, we sought to explore the possibility of detecting the immobilization of multiple peptides on the same platform and to study the selectivity of their binding properties. To achieve the co-immobilization of peptides CLPLGNSH (**2**) and CLRGRYW (**3**) the procedure as depicted in Scheme 2 was followed. First, fluorogenic coumarin **1** was immobilized by μCP in patterns consisting of 100 μm wide lines separated by 100 μm followed by the printing of peptide **2** in a 1 h step. To this end, a PDMS stamp with dots of 100 μm in diameter and separated by 100 μm was inked with a 10 mM solution of **2** in PBS for 30 min and placed in conformal contact with the functionalized substrates for 1 h. Subsequently, the substrates were incubated in a solution containing 10 mM of peptide **3** in order to backfill the unreacted regions of fluorogenic **1**. Finally, the bifunctional peptide surfaces were exposed to a solution containing both TGF-β1 (1 μg mL^{-1}) and BCII (50 μg mL^{-1}) and inspected using fluorescence microscopy subsequent to immunofluorescence staining. The images are presented in Fig. 2. Initially, patterns of **1** showed quenched coumarin fluorescence in agreement with our previous results (Fig. 2a). The coumarin fluorescence intensity is then regioselectively restored upon printing the first peptide **2** as signaled by the fluorogenic platform (Fig. 2b). In this case, the intensity of **1** was restored only in the printed dots that matched with patterned lines of **1** indicating the success of the Michael addition reaction. An incubation step with the second peptide **3** led to a recovery of the coumarin intensity in the remaining areas resulting in observing a continuous blue fluorescent line pattern of coumarin **1** (Fig. 2c). Upon close inspection, the 100 μm dots of **2** were still distinguishable in agreement with the larger enhancement of the coumarin intensity when compared to immobilizing **3** as observed above. Subsequently, the platform co-functionalized with the two peptides was incubated with a solution containing both TGF-β1 (1 μg mL^{-1}) and BCII (50 μg mL^{-1}) for 1 h (see ESI†). After rinsing, an immunostaining assay was performed against TGF-β1 (red) (Fig. 2e) yielding a clear match with the patterned regions of peptide **2** while the remaining areas were undistinguishable from the background (Fig. 2d). Then, an immunostaining assay was performed against BCII. From the recorded fluorescence images, green areas were observed that coincide with the remaining areas of the initial blue line pattern (Fig. 2e–g).

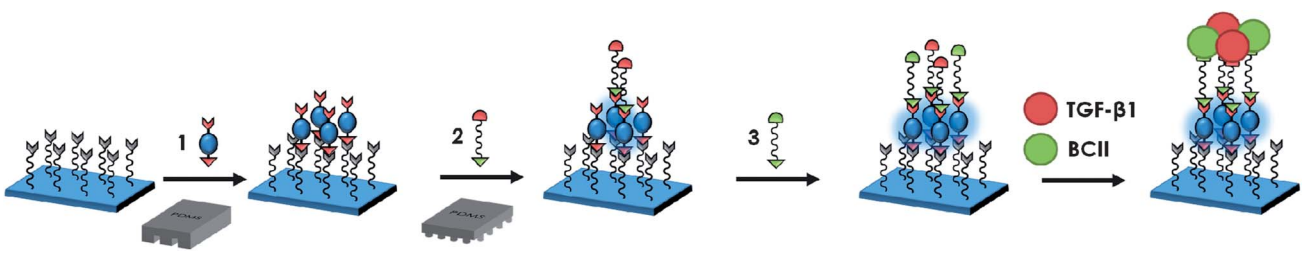

Scheme 2 Surface functionalization by a reactive μCP of **1** on an azide-terminated SAM followed by immobilization of **2** by reactive μCP as reported by the fluorogenic reaction, and subsequent immobilization of **3** by incubation. The bifunctional platforms were then incubated in a solution containing both TGF-β1 and BCII for 1 h and immunostained accordingly (see ESI†).

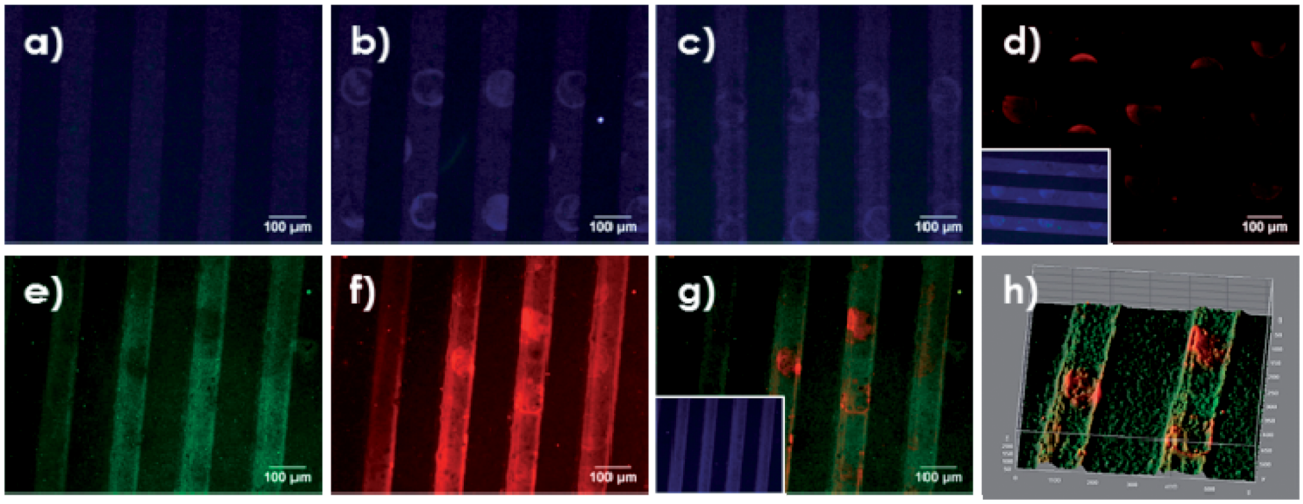

Fig. 2 (a–h) Fluorescence images of (a) a pattern of **1**, (b) the subsequent printing of **2** and (c) after incubation with **3**. (d) shows the immunostaining of TGF-β1 (red) after the platforms were incubated with a mixture containing both TGF-β1 and BCII and (e and f) show the platforms after immunostaining of BCII (green) using (e) the green or (f) the red channels. (g) is the overlay image of both (e) and (f) and (h) is the 3D surface plot corresponding to (g). Insets show the image taken using the blue channel while the main image was taken using either the red or the green channels.

When overlaying both fluorescence images the TGF-β1 and BCII regions could be clearly observed while the intensity of the coumarin pattern was fully restored (Fig. 2g). Therefore, the self-reporting surface resulted in an excellent tool to visualize the local step-wise peptide immobilization with the subsequent protein self-sorting of a mixture. In addition, this novel finding opens the possibility to combine both targeting and regenerative properties in a unique layer.

In another experiment the approach presented in Scheme 2 was followed using the same stamp with line features for all the surface functionalization steps (Fig. 3). In this manner, after cross-printing peptide **2** on patterns of coumarin **1**, the functionalized regions are equal in size and shape as compared to the reactive background. Upon incubation with the second peptide (**3**) a rise in fluorescence was observed in the initially dark regions, however two fluorescent regions were distinguished from the fluorescent intensity profiles along the lines of coumarin **1** (Fig. 3c).

This observation can be used to evaluate the specific binding of TGF-β1 and BCII to the correct peptide areas. After immunostaining the bifunctional platforms for TGF-b1 and BCII, a clear confinement of TGF-β1 was observed in regions functionalized with **2** while BCII was bound to regions functionalized with **3** (Fig. 3f).

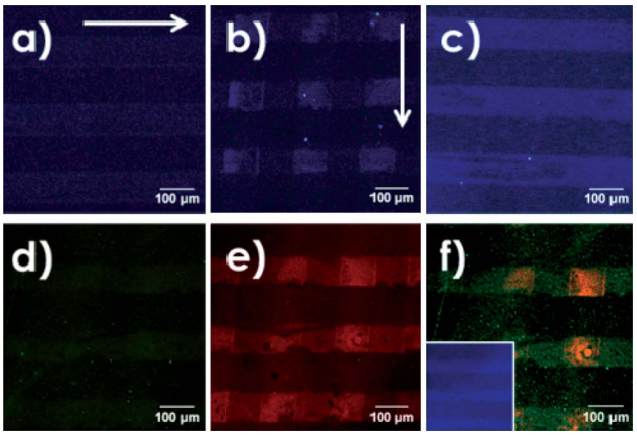

Fig. 3 Fluorescence images of (a) a pattern of **1**, (b) the subsequent cross-printing of **2** (arrows indicate printing direction) and (c) after incubation with **3**. (d) and (e) show the immunostaining of BCII (green) and TGF-β1 (red) respectively after the platforms were incubated with a mixture containing both proteins. (f) is the overlay image of both (d) and (e). Inset in (f) shows the image recorded using the blue channel.

Regenerative potential of platforms functionalized with CLPLGNSH

To demonstrate the biological activity of bound TGF-β1, a platform was fabricated that consisted of a full layer of peptide **2**. After printing **1** on an azide-terminated SAM using a flat featureless PDMS stamp, the fluorogenic surface was incubated with either a solution containing **2** or **2′**. The increase in the fluorescence intensity (Fig. 4a–c) indicates that the peptides were successfully immobilized. These platforms were then incubated with TGF-β1 (100 ng) and used for culturing human articular chondrocytes (HACs) for one week and the cellular morphology was analyzed (Fig. 4b–j). After 7 days, cells cultured in the absence of TGF-β1 exhibited an elongated morphology, which resembles a fibroblast-like phenotype.[15] Although a similar spreading behavior was observed irrespective of the surface in the absence of TGF-β1, higher numbers of adhered cells were observed on surfaces functionalized with **1** or peptide when compared to the bare azide-SAM (Fig. 4k–n). In contrast, those cultured in the presence of TGF-β1, either bound or supplemented in the culture medium, showed a more round to polygonal morphology, which better resembles a chondrocyte-like phenotype. In addition, the presence of pre-chondrogenic

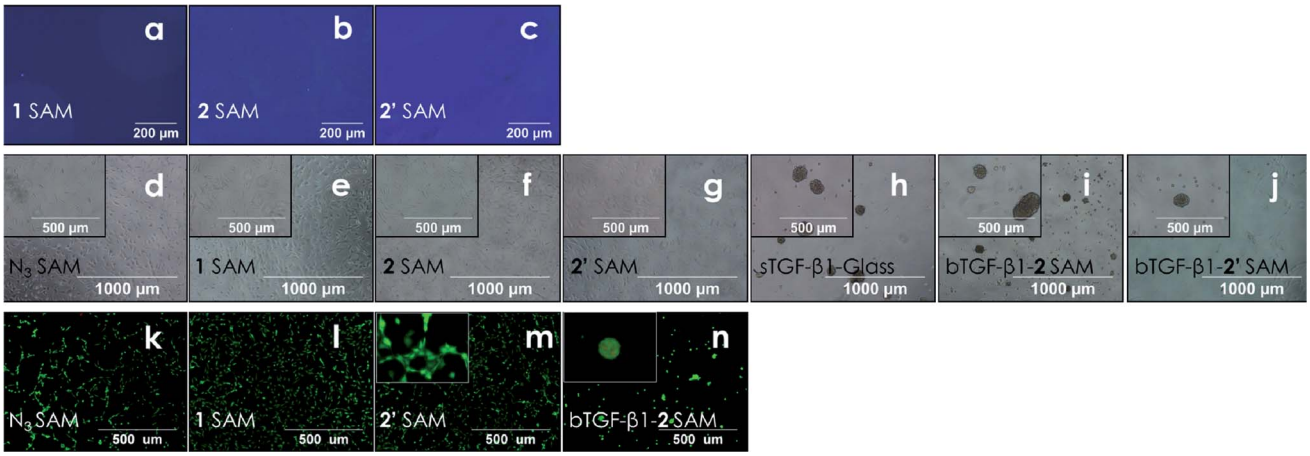

Fig. 4 (a–c) Fluorescence images corresponding to the functionalization of an azide-terminated SAM with **1** using a flat PDMS stamp and after incubation with **2** and **2′**. (b–j) HACs morphology after 7 days on the different functionalized substrates by bright field microscopy. sTGF-β1 refers to soluble (s) growth factor while bTGF-β1 indicates bound (b) protein. (k–n) Live–dead assay showing HACs seeded on different functionalized substrates.

cell condensations was observed as an early skeletogenesis event, common in cultures supplemented with TGF-β1.[16] These cellular condensations ranged in size and number being maximized for cells cultured on platforms of **2** with bound TGF-β1, followed by cells seeded on a glass slide with TGF-β1 (100 ng) supplemented in the medium while cells seeded on a platform of **2′** pre-loaded with 100 ng of growth factor showed the fewest and smallest cell condensations of them all.

These results not only show again that platforms of surface-bound **2** are useful for the binding with TGF-β1 but also that the growth factor remains active and is readily accessible for interacting with specific cellular receptors. When comparing the case when the same amount of TGF-β1 was delivered in solution, the observed stimulation in the case of TGF-β1 bound to **2** was enhanced, which could be related to a higher local concentration of growth factor at the surface. The enhanced stimulation led to larger sizes and higher quantities of cell condensations. These observations were in agreement with the literature[16,17] and the observations made on platforms with immobilized **2′**. In this case reduced sizes and quantities of pre-chondrogenic cell condensations were observed when compared to those with bound **2**. This indicates that the presence of TFG-β1 was important and confirms the specific binding between peptide **2** and TGF-β1. After performing a Live/Dead assay after 7 days of culture (Fig. 4k–n), the same cell morphologies were observed for the different cases while negligible cytotoxicity was observed.

From the analysis of the glycosaminoglycan (GAG) levels in HAC lysates after 7 days (Fig. 5a) a significantly higher production of GAGs by HACs was observed in the case where HACs were seeded on platforms of **2** with bound TGF-β1 when compared to the growth factor delivered in solution to cells seeded on glass or platforms with the peptide only. Interestingly, the presence of growth factor in the medium did not result in an enhanced GAG production by cells seeded on glass when compared with a negative control lacking TGF-β1. Taking into account that the relative induction of the GAG content for the highest value is only 1.4 fold, this effect could be attributed to the short duration of the experiment. In addition, HACs were stained for GAGs after 7 days with Alcian blue (Fig. 5b and c). Whereas the staining of cells seeded on platforms functionalized with peptide **2** was of low intensity in the absence of TGF-β1, cells cultured on platforms of peptide **2** that were incubated with TGF-β1 presented an intense color after staining, indicating a higher production of GAGs.

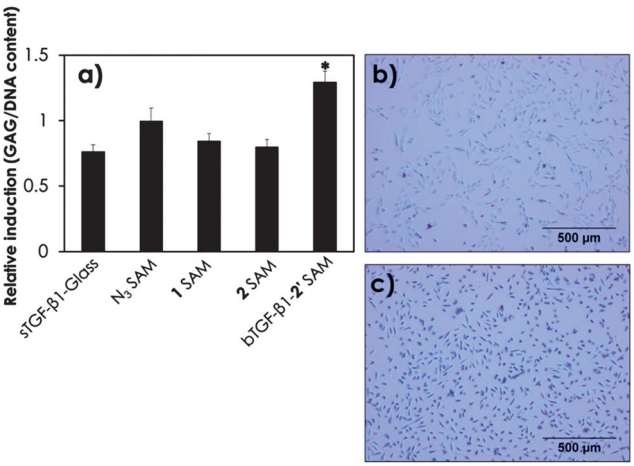

Fig. 5 (a) GAG levels normalized by the total DNA content of HACs after 7 days of culture, expressed as relative induction with respect to an azide-terminated SAM. (b) Alcian blue staining of cells seeded on **2** without (b) or with (c) TGF-β1.

Conclusions

In conclusion, a fluorogenic platform was successfully used to detect the chemoselective immobilization of different cysteine-terminated peptides with relevant properties in terms of cell adhesion and regeneration. We initially detected the immobilization of TGF-β1 and collagen-II as confirmed by the confinement of stained proteins within the fluorescent reporter

patterned regions. In addition, after analyzing specificity and cross-reactivity in terms of protein binding, biological properties could be combined by co-immobilizing two different peptide sequences at different parts on a single substrate. The co-immobilized peptides were able to selectively capture their envisioned protein binding partners TGF-β1 and BCII from a mixture. Incorporation of the fluorogenic coumarin can be achieved after a mild plasma oxidation step of biomaterials such as PLLA or PCL, which allows for installing the azide-terminated monolayer upon silanization. Therefore our methodology represents a novel strategy for visualizing the functionalization of existing biomaterials with functional biomolecules.

Notes and references

1 For reviews see for example: (*a*) S. W. O'Driscoll, *J. Bone Jt. Surg.*, 1998, **80**, 1795; (*b*) J. S. Temenoff and A. G. Mikos, *Biomaterials*, 2000, **21**, 431.
2 For reviews see for example: (*a*) G. P. Smith and V. A. Petrenko, *Chem. Rev.*, 1997, **97**, 391; (*b*) J. Scott and G. Smith, *Science*, 1990, **249**, 386.
3 For reviews see for example: (*a*) T. Aida, E. W. Meijer and S. I. Stupp, *Science*, 2012, **335**, 813; (*b*) H. Cui, M. J. Webber and S. I. Stupp, *Pept. Sci.*, 2010, **94**, 1.
4 For example: (*a*) R. N. Shah, N. A. Shah, M. M. Del Rosario Lim, C. Hsieh, G. Nuber and S. I. Stupp, *Proc. Natl. Acad. Sci. U. S. A.*, 2010, **107**, 3293; (*b*) M. J. Webber, J. Tongers, C. J. Newcomb, K. T. Marquardt, J. Bauersachs, D. W. Losordo and S. I. Stupp, *Proc. Natl. Acad. Sci. U. S. A.*, 2011, **108**, 13438.
5 D. A. Rothenfluh, H. Bermudez, C. P. O'Neil and J. A. Hubbell, *Nat. Mater.*, 2008, **7**, 248.
6 A. P. Hollander, I. Pidoux, A. Reiner, C. Rorabeck, R. Bourne and A. R. Poole, *J. Clin. Invest.*, 1995, **96**, 2859.
7 J. S. Dounchis, R. S. Goomer, F. L. Harwood, M. Khatod, R. D. Coutts and D. Amiel, *J. Orthop. Res.*, 1997, **15**, 803.
8 B. Johnstone, T. M. Hering, A. I. Caplan, V. M. Goldberg and J. U. Yoo, *Exp. Cell Res.*, 1998, **238**, 265.
9 C. Nicosia, J. Cabanas-Danés, P. Jonkheijm and J. Huskens, *ChemBioChem*, 2012, **13**, 778.
10 M. Heggli, N. Tirelli, A. Zisch and J. A. Hubbell, *Bioconjugate Chem.*, 2003, **14**, 967.
11 N. Balachander and C. N. Sukenik, *Langmuir*, 1990, **6**, 1621.
12 D. I. Rozkiewicz, D. Jańczewski, W. Verboom, B. J. Ravoo and D. N. Reinhoudt, *Angew. Chem., Int. Ed.*, 2006, **45**, 5292.
13 L. Yi, H. Li, L. Sun, L. Liu, C. Zhang and Z. Xi, *Angew. Chem., Int. Ed.*, 2009, **48**, 4034.
14 H. A. Behanna, J. J. J. M. Donners, A. C. Gordon and S. I. Stupp, *J. Am. Chem. Soc.*, 2005, **127**, 1193.
15 M. Schnabel, S. Marlovits, G. Eckhoff, I. Fichtel, L. Gotzen, V. Vécsei and J. Schlegel, *Osteoarth. Cart.*, 2002, **10**, 62.
16 (*a*) A. M. DeLise, L. Fischer and R. S. Tuan, *Osteoarth. Cart.*, 2000, **8**, 309; (*b*) H. J. Kwon, *Biochem. Biophys. Res. Commun.*, 2012, **424**, 793.
17 L. Wu, H. J. Prins, M. Helder, C. A. van Blitterswijk and H. B. J. Karperien, *Tissue Eng., Part A*, 2012, **18**, 1542–1551.

